

Dynamic object-based encoding and automatically prioritized position encoding in visual working memory

Zitong Lu^{1,2,3}, Hui Chen⁴, Yixuan Ku^{1,2,3} *

1. Guangdong Provincial Key Laboratory of Social Cognitive Neuroscience and Mental Health, Department of Psychology, Sun Yat-sen University, Guangzhou, China.

2. Peng Cheng Laboratory, Shenzhen, China.

3. Shanghai Key Laboratory of Brain Functional Genomics, Shanghai Changning-ECNU Mental Health Center, School of Psychology and Cognitive Science, East China Normal University, Shanghai, China.

4. Department of Psychology and Behavioral Sciences, Zhejiang University, Hangzhou, China.

* correspondence: Yixuan Ku, kuyixuan@mail.sysu.edu.cn

ResearcherID: D-4063-2018

ORCID: 0000-0003-2804-5123

Running title: Dynamic object-based encoding in VWM

ABSTRACT

Whether visual working memory (VWM) retains information from different features independently or as a unified object representation remains debated. Although behavioral studies have provided evidence that the unattended feature of a target could also be encoded in VWM, there still lacks neural supports for the object-based encoding. Here participants were asked to perform three VWM tasks (Orientation-Position, Position-Orientation, or Orientation-Color). They needed to recall the former feature as a task-relevant feature while the latter was a task-irrelevant feature combined with the task-relevant feature in the same object. Electroencephalogram (EEG) was recorded and decoded to track the representation of the task-relevant and task-irrelevant visual features dynamically. Orientation could be decoded more accurately as a task-relevant feature than a task-irrelevant feature. However, position could be decoded equally well in the task-relevant or task-irrelevant conditions, and the feature decoding accuracy of task-irrelevant position was even higher than the task-relevant orientation. Meanwhile, task-irrelevant color was not prioritized over task-relevant orientation. Importantly, there existed significant correlation between task-relevant and task-irrelevant features decoding accuracies across three VWM tasks, supporting the object-based coding hypothesis. The decoding accuracies of task-irrelevant features in all three conditions decreased in the second half of trials, while the correlation between decoding accuracies of relevant and irrelevant features only decreased in the orientation-color condition. Altogether these results suggested dynamic object-based encoding processes in VWM, yet, position, as a prioritized feature, could be encoded in a more automatic way.

SIGNIFICANCE STATEMENT

Visual working memory is connecting perception and high-level cognitive functions. Understanding what the fundamental encoding unit is in visual working memory and how visual features and objects are represented in human brain are essential questions in the field. Although behavioral studies suggested that task-irrelevant features were encoded in visual working memory, it was still unclear how they were assembled with task-relevant features. Here, electroencephalogram (EEG) decoding revealed a dynamic object-based encoding mechanism in visual working memory that the task-irrelevant feature was encoded together with task-relevant features at first but dropped later. Meanwhile, position as a prioritized feature was automatically encoded. Using decoding methods is a way to probe dynamic changes of representations of different features in perception and memory.

INTRODUCTION

Visual working memory (VWM) is one of the most critical functions for human cognition (Luck & Vogel, 2013). It is positively correlated with fluid intelligence and determines learning efficiency, mental calculation, reasoning, language learning, and other cognitive abilities. Many studies have revealed cognitive and neural mechanisms underlying VWM (Christophel et al., 2017; Luck & Vogel, 2013). Nevertheless, how memories of visual features are represented dynamically in the brain remains debated. The object-based coding hypothesis proposes that object is the primary storage unit for maintaining VWM (Gao et al., 2011; Hyun et al., 2009; Luck & Vogel, 1997; Luria & Vogel, 2011; Quinlan & Cohen, 2011; Shen et al., 2013; Vogel et al., 2001; Yin et al., 2012). Both task-relevant and task-irrelevant features of an object are encoded in the brain. In contrast, the feature-based coding hypothesis contends that all features are independently stored in capacity-limited sub-systems (Maunsell & Treue, 2006; Olson & Jiang, 2002; Wheeler & Treisman, 2002). Although previous studies have found behavioral evidence to support one of the two viewpoints, there still lack direct neural evidence and it is challenging to dynamically track memory representations over time in the human brain.

Traditional univariate analysis of neuroimaging studies on neural correlates of VWM (Baddeley, 2003; Nee et al., 2013) is less sensitive to reveal hidden neural patterns compared with multivariate pattern analysis (MVPA) (Norman et al., 2006). Task-relevant visual features during VWM such as orientation, position, and color can be decoded from signals of functional magnetic resonance imaging (fMRI) (Cai et al., 2019; Christophe et al., 2012; Ester et al., 2009, 2013, 2015; Gosseries et al., 2018; Harrison & Tong, 2009; Rose et al., 2016; Serences et al., 2009; Sprague et al., 2016), electroencephalograph (EEG) (Bae & Luck, 2018, 2019b; Bocincova & Johnson, 2019; Rose et al., 2016; Wolff et al., 2015, 2017; Xing et al., 2013), and magnetoencephalography (MEG) (Quentin et al., 2019). Yet, task-irrelevant features have rarely been investigated during VWM processes, which would contribute to the resolution of the debates mentioned above. If both the relevant and irrelevant features could be successfully decoded during encoding and maintenance periods and the decoding accuracies are correlated, the object-based coding hypothesis would be supported. Otherwise, if only the relevant features could be decoded, or if the irrelevant features could also be decoded but its decoding accuracy has no relationship with the relevant feature, it suggests independence of the relevant and irrelevant features, and the feature-based coding hypothesis was supported.

Thus, in the present study, we conducted an EEG experiment with three VWM tasks (Orientation-Position, Position-Orientation, or Orientation-Color) to test the above hypotheses, with the former feature as a task-relevant feature while the latter was a task-irrelevant feature combined with the task-relevant

feature in the same object. Using MVPA methods to decode features from EEG signals, the representation of task-relevant and task-irrelevant features was tested dynamically over time. First, both task-relevant and task-irrelevant features in all three tasks could be successfully decoded, and the decoding accuracies were significantly correlated between task-relevant and task-irrelevant features, which supported the object-based coding hypothesis. Second, position could be decoded better than orientation and color, no matter if it is a task-relevant or task-irrelevant feature, confirming spatial location as a prioritized feature in visual processing (Chen & Wyble, 2015; Pertzov & Husain, 2014; A. M. Treisman & Gelade, 1980; A. Treisman & Zhang, 2006; Wheeler & Treisman, 2002). Third, decoding accuracies of all task-irrelevant features and correlations between task-relevant orientation and task-irrelevant color decreased as task went on, suggesting a dynamic object-based theory that our brain encoded both the relevant and irrelevant features of an object together at the beginning but dropped the irrelevant feature later. Yet, such dropping was not observed for position, further suggesting position as a prioritized feature and processed in an automatic way.

MATERIALS AND METHODS

Participants

Six students from East China Normal University between the ages of 21 and 24 (3 male and 3 female, age = 22.67 ± 1.49) with normal or corrected-normal visual acuity participated in all the experiments. All six participants had no history of mental illness and were compensated for their time after the experiment. Written informed consent was provided by all participants before the experiment. Similar to previous studies (Hogendoorn & Burkitt, 2018; Stansbury et al., 2013; Zhan et al., 2019), we collected more data from less participants. Each participant here completed experiments in 2-5 days according to their mental state and all of them performed the tasks for over ten hours in total. All experimental protocols and informed consents were approved by the Institutional Review Board of East China Normal University.

Stimuli and apparatus

Participants were asked to perform three kinds of tasks (**Figure 1**). All stimuli were generated by Psychtoolbox based on MATLAB. Participants were seated on a chair 63cm far from the screen with their heads fixed using a chin rest.

Task 1 is an Orientation-Position VWM task. Participants were asked to memorize the orientation of a grating, ignoring the position information. During the experiment, each trial begun with a sample grating (visual angle 5°) displayed randomly on the left or right side (50% probability each) of the screen for 0.5s. The grating orientation was set to 23° , 158° , or a random angle

different from the two (the ratio of the three conditions is 1:1:1). Following a delay period of 2s, a probed grating with a random orientation would be presented at the same position as the sample grating. Participants were requested to recall the sample grating orientation as precisely as possible by using a mouse to rotate the grating.

Task 2 is a Position-Orientation VWM task. Participants were asked to memorize the position of a grating, ignoring the orientation information. During the experiment, each trial began with a sample grating (visual angle 5°) with the orientation of 23° or 158° randomly (50% probability each) displayed on a fixed position on the left side or a fixed position on the right side or a random position different from the two fixed position on the screen for 0.5s. The ratio of the three position conditions is 1:1:3. In this task, two fixed conditions was easier to realize for participants. Thus, we increased the number of random trials so that the participant could hardly perceive the fixed positions. Following a delay period of 2s, a probed grating with the same orientation as the sample grating would be presented at a random position. Participants were requested to recall the memorized grating position as precisely as possible by using the mouse to move the grating.

Task 3 is an Orientation-Color memory task. Participants were asked to memorize the orientation of a grating similar to task 1, ignoring the color information. During the experiment, each trial began with a sample grating (visual angle 5°) with the color of red or green randomly (50% probability each) displayed on the screen center for 0.5s. The grating orientation was set to 38° , 143° , or a random angle different from the two (the ratio of three conditions is 1:1:1). Following a delay period of 2s, a probed grating with a random orientation would be presented at the center of the same color as the sample grating. Participants were requested to recall the sample grating orientation as precisely as possible by using the mouse to rotate the grating.

The inter-trial interval of all three tasks was set from 1s to 1.3s randomly. Each block consisted 60 trials and last for approximately 450s. Each participant completed at least 15 blocks (15-18 for each participant) of task 1 and at least 25 blocks (25-28 for each participant, in order to control the same number of trials of two fixed positions as the number of trials of two fixed orientations in other two tasks) of task 2 and at least 15 blocks (15 to 18 for each participant) of task 3. Each participant received at least 10 practice-trials for each task and performed at least 3300 task-trials in total. The order of the blocks was randomly presented to participants.

EEG recording and preprocessing

The continuous EEG was recorded using a Brain Products recording system, with 64 channels embedded in a cap according to the international 10/20 system. The impedance of all channels was kept below 10 k Ω during recording. EEG signals were sampled with a frequency of 250 Hz. EEGLAB

toolbox ([Delorme & Makeig, 2004](#)) was used to preprocess the data.

All channels were re-referenced offline to the averaged mastoids through the signal recorded from channels TP9 and TP10. EEG data were filtered by 0.1 Hz high-pass and 40 Hz low-pass and then divided into segments ranging from 500ms before to 3000ms after the presentation of the sample display. Independent component analysis (ICA) was then performed on the scalp EEG for each participant to identify and remove components that were associated with blinks ([Jung et al., 2000](#)) and eye movements ([Drisdelle et al., 2017](#)). The trials of the two fixed orientations in task 1 and task 2 and the two fixed positions in task 3 were used for subsequent analysis.

Decoding Analysis

The implementation of the decoding analysis (including classification training and test) was based on Python. We attempted to decode relevant features and irrelevant features in our three tasks, including orientation (as a relevant feature in task 1 and task 2, as an irrelevant feature in task 3), position (as a relevant feature in task 1, as an irrelevant feature in task 3) and color (as an irrelevant feature in task 3).

Following the procedures in previous studies (Bae & Luck, JN, 2018), EEG signals limited in frequencies between 2 Hz and 6 Hz, and EEG signals in the alpha band which was bandpass filtered at 8-12 Hz and computed the magnitudes of the complex analytic signals by a Hilbert transform were used in decoding analysis. In all decoding cases, the data were resampled by a 20ms time-window, which contained 5 time-samples. Each participant got six 4-dimensional data matrices for each of the six visual features in three tasks, with dimensions of time (175 time-windows), channels (64 channels), trials (at least 600 trials), patterns (the two fixed conditions, e.g., two fixed orientations in task 1).

Linear support vector machine (Linear-SVM) was selected to conduct a classification of the visual feature of the two conditions across time for each participant. Pattern labels were binarized first and five-fold cross-validation procedure was then used to assess how well the patterns could be dissociated from the EEG data. Data from 80% trials (selected randomly) were used to train the Linear-SVM classifier based on the pattern labels. The remaining trials were then used to test the performance of the classifier. We also trained the classifier from data in one time-window and tested it from data in another time-window. This classification steps were repeated 100 times for each time-by-time point with a different random-selecting-seed for dividing the trials to get a more reliable result, and the classification accuracies were then averaged. We conducted the decoding process for each feature of tasks individually, and the values from different participants were statistically analyzed. All the classification program was implemented based on *svm* and *model_selection* modules in scikit-learn ([Pedregosa et al., 2011](#)) by Python.

To further check the reliability of VWM representations across participants and exclude the potential strategic differences between participants, we mixed data from all participants with over 20,000 trials in each condition and performed an across-participants decoding following the same protocol as for individuals, with the five-fold cross-validation procedure and 100 iterations. The test accuracies of the 100 iterations were then used for statistical analysis.

Statistical analysis

Suppose the neural representational pattern of a certain time contains encoding a specific visual feature in the brain. In that case, the decoding accuracy should be greater than chance, which was 50%, because we have two categories in our decoding processes. To compare decoding accuracy for a feature in a task to chance at each decoding time point, we used a permutation test for comparing the distributions corresponding to decoding accuracies and the chance level to assess statistical significance. This means that we randomly shuffled decoding accuracies and chance accuracies (50%). Then, we calculated the results for 5000 iterations to draw a distribution. Real accuracies exceeding 95% of the distribution are regarded as significant. *P*-values were calculated from this permutation distribution.

For the cross-temporal decoding results, we used the cluster-based permutation test to assess statistical significance. First, we calculated *t*-values for each time-point comparing to the chance level and extracted each significant cluster. And we calculated the clustering statistic as the sum of *t*-values in each cluster. Then we conducted 5000 permutations to calculate the maximum cluster statistic for each iteration and obtained a distribution of maximum permutation cluster statistic. Finally, we assigned *p*-values to each cluster of the actual decoding accuracies by comparing its cluster statistic with the permutation distribution.

RESULTS

Behavioral performance

Observed behavioral performances were excellent in all three tasks. In Orientation-Position task and Orientation-Color task, accuracy on each trial was quantified as the angular difference between the orientation of the sample grating and the orientation reproduced by the participant. In Position-Orientation task, accuracy on each trial was quantified as the distance between the position of the center of the sample grating and the position of the center of the grating reproduced by the participant. The mean absolute errors were quite small in three tasks (Orientation-Position task: 8.92°, SEM=0.95; Position-Orientation task: 40.39 pixels, SEM=4.88; Orientation-Color task: 8.63°, SEM=1.04).

Orientation and position decoding in task 1 and task 2

Firstly, we decoded the orientation and position in both orientation-position task and position-orientation task time-by-time. In the former, the orientation was the task-relevant feature, and the position was the task-irrelevant feature. In the latter, they were converse. The ERP time-by-time classification performances of both orientation and position in these two tasks are shown in **Figure 2a and 2b**. These decoding results showed that both orientation and position could be successfully decoded in the stimulus period, delay period, and response period, whether as the task-relevant feature or the task-irrelevant feature. However, the position was easier to decode in both tasks that the classification accuracy of position was higher than orientation and had longer significant periods than orientation.

Although we could hardly detect whether the participant had memorized the irrelevant feature through the behavioral indicator, we successfully used decoder to decode the irrelevant feature. It proved a mechanism of storing object information, including orientation and position in our brains in VWM.

We then calculated the difference in decoding accuracies between the same feature being relevant or irrelevant (**Figure 2c**). The results showed that the decoding performance of the task-relevant orientation was significantly higher than the task-irrelevant orientation during 300-400ms, 900-1100ms, and 2200-2600ms. On the contrary, the decoding performances of the relevant position and the irrelevant position were hardly different. However, the feature decoding accuracy of task-irrelevant position was even higher than the task-relevant orientation (**Figure 2d**).

Moreover, we conducted a series of cross-temporal decoding processes on orientation and position in task 1 and task 2. We input ERP data at different time-points to train the classifier and used this trained-classifier at a certain time-point to test the data at all time-points on the time series. If the classifier trained on certain time-point's data could be a good predictor of brain activity at another time, this meant the memory representations at these two time-points were highly consistent. The cross-temporal decoding results not only reflected the time-by-time results but also reflected the continuity and consistency of feature coding in a task.

Figure 3a shows the temporal generalization decoding results by cross-temporal decoding in task 1 and task 2. Whether as the relevant feature in task 2 or as the irrelevant feature in task 1, the position had strong coding persistence during the delay period. Orientation had coding consistency in the early stage of delay while as the relevant feature in task 1. When orientation was the irrelevant feature in task 2, the decoding results were only significantly higher than the random level during the stimulus period and early delay period. The poor continuity of their coding patterns meant that only the predictor trained and test on very close time had a significantly higher decoding accuracy.

These decoding results demonstrated that there were different coding

formats between different irrelevant features in VWM. Position might be a stronger feature than orientation in VWM, which can be automatically prioritized encoded. Whether the position is regarded as a relevant or irrelevant feature, the brain had strong coding for spatial information. In contrast, orientation might be a weaker feature. When orientation is the relevant feature in the task, the brain had more robust coding for orientation information. However, when orientation was the irrelevant feature, its coding became weak.

Orientation and color decoding in task 3

As the task-irrelevant feature in VWM, we could decode position better than orientation. Color is also one of the basic features of vision. Here we would like to test how color is represented in our brain as an irrelevant feature. We hypothesized that color and orientation were features of the same kind and position were a unique feature, so the decoding results of color as the irrelevant feature would be similar to task-irrelevant orientation.

First, we conducted the time-by-time decoding process on orientation and color in task 3. The time-by-time classification performances show that both the task-relevant feature (orientation) and the task-irrelevant feature (color) were coded in this task. Both decoding accuracies were significantly higher than chance during the stimulus period, early delay period, and the response period (**Figure 2e and 2f**). Then, we conducted the cross-temporal decoding for orientation and color in task 3. **Figure 3b** shows that the cross-temporal decoding result of orientation is similar to orientation as the relevant feature in task 1. The cross-temporal decoding result of color is similar to the result of orientation as the irrelevant feature in task 2.

We found that the brain represented irrelevant features of three different visual features in all three tasks using ERP decoding. Our dynamic decoding results powerfully demonstrate the object-based encoding mechanism in VWM. Although the decoding results of orientation and color in this task were similar to the previous time-by-time results, it could be seen from the cross-temporal analysis that color, as an irrelevant feature, had very weak coding persistence and consistency. Combining orientation decoding results in task 2 and color decoding results in task 3, we found that both orientation and color are weak features. When these weak features were task-irrelevant in VWM, their coding was not so continuous that they could only be trained and successfully predicted by neural activities at closed time points. However, the position was a more powerful feature. Whether position was the relevant or irrelevant feature, the decoding results were similar with strong continuity and consistency.

Phased decoding in three tasks

To explore whether the coding pattern of visual features, both task-relevant and task-irrelevant features, would change as the experiment repeatedly went on, we conducted the phased decoding for visual features (both relevant and

irrelevant features) in three tasks. The trials in each task were divided equally into two parts: early phase and late phase according to the time sequence, and the features were decoded, respectively. The decoding process was the same as above.

We calculated the differences between the decoding results of the two phases (**Figure 5a**). It could be seen that the decoding performances of the relevant features in all three tasks were no significant difference between the two phases. However, the decoding performances of the irrelevant features in all three tasks were higher in the early phase than in the late phase in some periods (position in task 1: 600-400ms, 2300-2500ms; orientation in task 2: 300-500ms, 650-700ms, 2600-2700ms; color in task 3: 0-150ms, 350-550ms, 2500-2600ms).

These phase decoding results demonstrated that when the participant memorized one single feature (the relevant feature) in a VWM task, the irrelevant feature would also be encoded from the start. Furthermore, as the experiment continues, we did not see a decrease in synchronization of both the relevant and irrelevant features or a rise of the relevant feature and fall of the irrelevant feature. It is only the coding of the irrelevant feature instead of the relevant feature in the brain that would gradually weaken. These results suggested that the task-relevant feature and the task-irrelevant feature had two independent different coding patterns in our brains. Besides, this reduction of the task-irrelevant feature was more substantial for encoding position information than other features, such as orientation or color, possibly because position was easier to decode.

Correlations between the relevant and irrelevant features

Since we had decoded various features successfully, we further confirmed the object-based hypothesis by correlation analysis. Here, we calculated the correlations (Spearman correlation coefficients) of decoding accuracies between the task-relevant and task-irrelevant features in three tasks. Giving the decoding accuracies from the sample period to the response period (0-3000ms), we found that the decoding accuracies of the task-relevant and task-irrelevant features were significantly correlated in all three tasks (**Figure 4**). Then, we computed the correlations between two kinds of accuracies for the two phases (early and late) (**Figure 5b**). The early phase's correlations of all three tasks were significant. The correlations of orientation-position task and position-orientation task in the late phase were also significant. However, it was not significant for the late phase's correlation of orientation-color task. Also, there was no significant difference between the two phases.

On the one hand, the results suggested a synchronous integration mechanism to bind different features into an object in VWM. On the other hand, although there was no significant difference between the two phases, the mean values of the later phase's correlations were lower than the early phase. There

might be a weakening of the binding effect, and the consistency of the irrelevant feature to the relevant feature was destroyed in the orientation-color task. Besides, although the task-irrelevant feature's coding strength decreased, the consistency between the relevant and irrelevant features was still high. The sustaining consistency in orientation-position task and position-orientation task just went to show that position played an essential role in maintaining this bound mechanism that the irrelevant feature could be automatically encoded.

Across-participants decoding

Finally, to test whether different individual memory strategies influenced this object-based encoding phenomenon, we then decoded two corresponding visual features of each task across six participants. We conducted a similar classification process by inputting all participants' ERP data ten times. The final accuracy was the average of ten iterations. **Figure 6** shows the results, which are similar to that of single-participant decoding. Either the task-relevant or task-irrelevant feature could be successfully decoded.

It demonstrated that the decoding results of each visual feature were not affected by the differences in individual memory strategies. This mechanism of object-based representation in VWM was common and consistent in the human brain.

Alpha power decoding

Finally, we decoded the two kinds of features in three tasks based Alpha power. Both time-by-time and cross-temporal results can be seen in **Figure 7**. In contrast to ERP decoding, the alpha power decoding brought some differences. The decoding accuracies of position in both task 1 and task 3 were significantly higher than chance with strong continuity and consistency during stimulus period, delay period and response period, which was consistent with the results by ERP decoding. For other features' decoding accuracies, only the decoding accuracies of orientation as the task-irrelevant feature in task 3 during stimulus period and early delay period were significantly higher than the random level for short duration. The orientation as the task-relevant feature in task 1 and task 2 and the color as the task-irrelevant feature in task 2 could be hardly decoded by alpha power.

These demonstrated that alpha oscillations were mainly involved in encoding the information of position rather than orientation or color. Also, there might have a feature binding mechanism in the process of encoding position in alpha oscillations. In other words, when position as the task-relevant feature in a memory task, alpha power could not only encode position but also encode part of the task-irrelevant feature bended to position.

DISCUSSION

EEG decoding can be an efficient method to explore how information

dynamically represents in perception (Grootswagers et al., 2019; Hogendoorn & Burkitt, 2018; Mares et al., 2020; Noah et al., 2020; Robinson et al., 2019; Smith & Smith, 2019), mental imagery (Shatek et al., 2019; Xie et al., 2020), and memory (Bae & Luck, 2018, 2019b; Bocincova & Johnson, 2019; LaRocque et al., 2013; Wolff et al., 2015). Especially in the VWM task, it is difficult to effectively monitor how the brain encodes different low dimensional features at different times. EEG decoding can be an effective method to track the representations of object features dynamically. In our study, we attempted to decode the visual features time-by-time and compared the difference between classification accuracies and the random level at different time-points to evaluate the encoding of features in the memory process.

In our present study, we successfully decoded the task-relevant features of three different tasks. To our delight, we also successfully decoded all the task-irrelevant features. In some behavioral studies, participants had consistent performances between remembering single features and multi-feature objects in change detection tasks (Delvenne & Bruyer, 2004; Luck & Vogel, 1997; Olson & Jiang, 2002; Riggs et al., 2011). Some research also utilized the surprising test by a single surprise trial (Chen & Wyble, 2016; Shin & Ma, 2016; Swan et al., 2016), finding that participants could memorize the task-irrelevant feature. Our decoding results provided strong neural evidence that the task-irrelevant feature could be automatically encoded in our brains. Even, the across-participants time-by-time decoding showed same representational results for these features. Thus, the format of memory representations in our brains is object-based.

Some previous studies demonstrated that position as the task-irrelevant feature was automatically encoded into VWM (Jiang et al., 2000; A. Treisman & Zhang, 2006), while other nonspatial features as the task-irrelevant feature had no representation (Serences et al., 2009; Woodman & Vogel, 2008). However, our decoding results with large trials showed that even orientation and color were automatically encoded. In the meantime, the successful decoding of visual features occurred in the sample stage, the delay stage, and the response stage, which indicated that these object-based representations happened from the perception period to the maintenance period to the recall period.

Importantly, comparing the decoding results for different features, we concluded that our brains represented different features differently. Previous fMRI studies found that many regions, such as lateral PFC, frontal eye field, lateral intraparietal area and superior colliculus, were involved in encoding spatial information in VWM (Ester et al., 2015; Jerde et al., 2012; Rahmati et al., 2018, 2020; Riggall & Postle, 2012). In current EEG research, the decoding performances were lower for orientation and color than position. For the three different irrelevant features, position was significantly more powerful than orientation and color in terms of time-by-time decoding accuracies and cross-

temporal decoding results. Also, coding patterns of orientation and color information hardly had time persistence, while position had strong coding consistency in the whole task. These proved that position was a very powerful feature ([Chen & Wyble, 2015](#); [Pertsov & Husain, 2014](#); [A. M. Treisman & Gelade, 1980](#); [A. Treisman & Zhang, 2006](#); [Wheeler & Treisman, 2002](#)), while other visual features such as orientation and color were weak features. This might be the reason why we could hardly find evidence for the representation of task-irrelevant orientation or color by the behavioral performance and the ERP component such as contralateral delay activity (CDA). This super feature had similar strong coding under the two conditions by comparing the results of position as a relevant feature and an irrelevant feature. This indicated that the representation of position might not be affected by the task, and position might be the basis for integrating features into the object in VWM. There is an automatically prioritized position encoding mechanism in our brains.

Though the phased decoding benefited by the vast number of trials in our experiments, we compared representational differences between the early and late phases. A previous behavioral study ([Swan et al., 2016](#)) found that memory had different variable precisions for the task-relevant and the task-irrelevant features. Different precisions corresponding to different features were influenced by various degrees of attention. If, as it said, the attention became more focused on the relevant feature as the task progressed, the encoding of the relevant feature in the late phase would be stronger, and the encoding of the irrelevant feature would be weaker. However, our phased decoding results suggested that the irrelevant feature's coding strength would decrease as the task went on. There was no difference in the relevant feature's coding strength between the early and late. This process might not be because participants paid more attention to the task-relevant feature. On the contrary, there might be two independent representational patterns for the relevant and irrelevant features. When the participant only memorized one feature continuously in the same task, the relevant feature's encoding remained unchanged, but the irrelevant feature's encoding gradually weakened.

By calculating the correlation between decoding accuracies of the relevant and irrelevant features, we contended again that VWM was object-based encoding that the relevant and irrelevant features had consistent representations. Although the phased correlation results indicated no significant differences between the two phases, we could see a little tendency for the correlations between the two features to become weak, especially in the orientation-color task. Lacking position changes in the task and position as a unique feature strongly supporting feature integration into object could explain why the correlation between orientation and color was not significant in the late phase.

Profoundly exploring the coding mechanism through a very long experiment and EEG decoding method, we highlighted the dynamic object-based encoding

and the automatically prioritized position encoding in VWM. The foundational encoding unit of memory was the object. Thus, the object's task-irrelevant feature was automatically represented and bounded to the task-relevant feature in VWM. Furthermore, the irrelevant feature's coding strength but not the relevant feature would decrease if people continuously focused on one feature of the object in the task. In this dynamic object-based encoding process, the irrelevant feature binding the relevant gradually weakened with the relevant feature's coding staying the same. And position, as a prioritized feature, could be encoded automatically equally with in both relevant and irrelevant conditions. This helps us to understand further the processing and storage of memory in our brains.

Using Alpha power data to decode different visual features, only position had a good decoding result. This also verified the correlation between Alpha-band oscillation and spatial attention (Bae & Luck, 2018; Foster et al., 2017; van Ede et al., 2017; Worden et al., 2000). In addition, we found that when position was a variation feature in a VWM task (whether as the task-relevant or irrelevant), orientation could be weakly decoded. It is possible that Alpha band oscillation may also participate in a bit of encoding of features bound to position information.

However, there is still a lot more to explore about the binding of object features in VWM. First, in our current research, what we focused on was the integration of different kinds of features. Some previous studies found that objects containing two features from the same type had difficulty in remembering them in the form of the object (Delvenne & Bruyer, 2004; Olson & Jiang, 2002; Parra et al., 2011; Wheeler & Treisman, 2002; Xu, 2002). Because in this case, the participant would simultaneously view two features from the same type, it would be more difficult to decode than one feature corresponding to one feature type. Hence, we need to design more complex experiments to answer it from the perspective of neural decoding. Second, we should increase the memory load to evaluate the object-based mechanism under more complicated conditions. Thirdly, the storage mechanism of different features of real-world objects might be different with simple features (e.g., orientation, position and color) in memory (Utochkin & Brady, 2019). We need to apply the more complex and meaningful stimuli to explore the binding of object features in VWM. Finally, we also hope to use fMRI with a higher spatial resolution to see which regions dynamic processing the memory in our brains and further explain the dynamic object-based encoding process in the future.

ACKNOWLEDGEMENTS

We gratefully acknowledge the support of the National Social Science Foundation of China (17ZDA323), the Shanghai Committee of Science and Technology (19ZR1416700) and the Hundred Top Talents Program from Sun Yat-sen University to YK.

REFERENCE

- Albers, A. M., Kok, P., Toni, I., Dijkerman, H. C., & De Lange, F. P. (2013). Shared representations for working memory and mental imagery in early visual cortex. *Current Biology*, 23(15), 1427–1431.
<https://doi.org/10.1016/j.cub.2013.05.065>
- Baddeley, A. (2003). Working memory: Looking back and looking forward. *Nature Reviews Neuroscience*, 4, 829–839.
<https://doi.org/10.1038/nrn1201>
- Bae, G. Y., & Luck, S. J. (2018). Dissociable decoding of spatial attention and working memory from EEG oscillations and sustained potentials. *Journal of Neuroscience*, 38(2), 409–422.
<https://doi.org/10.1523/JNEUROSCI.2860-17.2017>
- Bae, G. Y., & Luck, S. J. (2019a). Decoding motion direction using the topography of sustained ERPs and alpha oscillations. *NeuroImage*, 184, 242–255. <https://doi.org/10.1016/j.neuroimage.2018.09.029>
- Bae, G. Y., & Luck, S. J. (2019b). Reactivation of Previous Experiences in a Working Memory Task. *Psychological Science*, 30(4), 587–595.
<https://doi.org/10.1177/0956797619830398>
- Ban, H., Preston, T. J., Meeson, A., & Welchman, A. E. (2012). The integration of motion and disparity cues to depth in dorsal visual cortex. *Nature Neuroscience*, 15, 636–643. <https://doi.org/10.1038/nn.3046>
- Bannert, M. M., & Bartels, A. (2013). Decoding the yellow of a gray banana. *Current Biology*, 23(22), 2268–2272.
<https://doi.org/10.1016/j.cub.2013.09.016>
- Bocincova, A., & Johnson, J. S. (2019). The time course of encoding and maintenance of task-relevant versus irrelevant object features in working memory. *Cortex*, 111, 196–209.
<https://doi.org/10.1016/j.cortex.2018.10.013>
- Chen, H., & Wyble, B. (2015). The location but not the attributes of visual cues are automatically encoded into working memory. *Vision Research*, 107, 76–85. <https://doi.org/10.1016/j.visres.2014.11.010>
- Chen, H., & Wyble, B. (2016). Attribute amnesia reflects a lack of memory consolidation for attended information. *Journal of Experimental Psychology: Human Perception and Performance*, 42(2), 225–234.
<https://doi.org/10.1037/xhp0000133>
- Christophel, T. B., Klink, P. C., Spitzer, B., Roelfsema, P. R., & Haynes, J. D. (2017). The Distributed Nature of Working Memory. In *Trends in Cognitive Sciences* (Vol. 21, Issue 2, pp. 111–124). Elsevier Ltd.
<https://doi.org/10.1016/j.tics.2016.12.007>
- Delorme, A., & Makeig, S. (2004). EEGLAB: An open source toolbox for analysis of single-trial EEG dynamics including independent component analysis. *Journal of Neuroscience Methods*, 134(1), 9–21.
<https://doi.org/10.1016/j.jneumeth.2003.10.009>
- Delvenne, J. F., & Bruyer, R. (2004). Does visual short-term memory store

- bound features? *Visual Cognition*, 11(1), 1–27.
<https://doi.org/10.1080/13506280344000167>
- Drisdelle, B. L., Aubin, S., & Jolicoeur, P. (2017). Dealing with ocular artifacts on lateralized ERPs in studies of visual-spatial attention and memory: ICA correction versus epoch rejection. *Psychophysiology*, 54(1), 83–99.
<https://doi.org/10.1111/psyp.12675>
- Ester, E. F., Sprague, T. C., & Serences, J. T. (2015). Parietal and Frontal Cortex Encode Stimulus-Specific Mnemonic Representations during Visual Working Memory. *Neuron*, 87(4), 893–905.
<https://doi.org/10.1016/j.neuron.2015.07.013>
- Fahrenfort, J. J., Grubert, A., Olivers, C. N. L., & Eimer, M. (2017). Multivariate EEG analyses support high-resolution tracking of feature-based attentional selection. *Scientific Reports*, 7, 1886.
<https://doi.org/10.1038/s41598-017-01911-0>
- Foster, J. J., Bsales, E. M., Jaffe, R. J., & Awh, E. (2017). Alpha-Band Activity Reveals Spontaneous Representations of Spatial Position in Visual Working Memory. *Current Biology*, 27(20), 3216–3223.e6.
<https://doi.org/10.1016/j.cub.2017.09.031>
- Gao, T., Gao, Z., Li, J., Sun, Z., & Shen, M. (2011). The Perceptual Root of Object-Based Storage: An Interactive Model of Perception and Visual Working Memory. *Journal of Experimental Psychology: Human Perception and Performance*, 37(6), 1803–1823.
<https://doi.org/10.1037/a0025637>
- Grootswagers, T., Robinson, A. K., Shatek, S. M., & Carlson, T. A. (2019). Untangling featural and conceptual object representations. *NeuroImage*, 202, 116083. <https://doi.org/10.1016/j.neuroimage.2019.116083>
- Hogendoorn, H., & Burkitt, A. N. (2018). Predictive coding of visual object position ahead of moving objects revealed by time-resolved EEG decoding. *NeuroImage*, 171, 55–61.
<https://doi.org/10.1016/j.neuroimage.2017.12.063>
- Hong, X., Bo, K., Meyyappan, S., Tong, S., & Ding, M. (2020). Decoding attention control and selection in visual spatial attention. *Human Brain Mapping*, 41(14), 3900–3921. <https://doi.org/10.1002/hbm.25094>
- Hyun, J. seok, Woodman, G. F., Vogel, E. K., Hollingworth, A., & Luck, S. J. (2009). The Comparison of Visual Working Memory Representations With Perceptual Inputs. *Journal of Experimental Psychology: Human Perception and Performance*, 35(4), 1140–1160.
<https://doi.org/10.1037/a0015019>
- Jerde, T. A., Merriam, E. P., Riggall, A. C., Hedges, J. H., & Curtis, C. E. (2012). Prioritized maps of space in human frontoparietal cortex. *Journal of Neuroscience*, 32(48), 17382–17390.
<https://doi.org/10.1523/JNEUROSCI.3810-12.2012>
- Jiang, Y., Olson, I. R., & Chun, M. M. (2000). Organization of Visual Short-Term Memory. *Journal of Experimental Psychology: Learning Memory*

- and Cognition*, 26(3), 683–702. <https://doi.org/10.1037/0278-7393.26.3.683>
- Johnson, M. R., & Johnson, M. K. (2014). Decoding individual natural scene representations during perception and imagery. *Frontiers in Human Neuroscience*, 8(1 FEB), 59. <https://doi.org/10.3389/fnhum.2014.00059>
- Jung, T. P., Makeig, S., Westerfield, M., Townsend, J., Courchesne, E., & Sejnowski, T. J. (2000). Removal of eye activity artifacts from visual event-related potentials in normal and clinical subjects. *Clinical Neurophysiology*, 111(10), 1745–1758. [https://doi.org/10.1016/S1388-2457\(00\)00386-2](https://doi.org/10.1016/S1388-2457(00)00386-2)
- Koch, G. E., Paulus, J. P., & Coutanche, M. N. (2020). Neural Patterns are More Similar across Individuals during Successful Memory Encoding than during Failed Memory Encoding. *Cerebral Cortex (New York, N.Y. : 1991)*, 30(7), 3872–3883. <https://doi.org/10.1093/cercor/bhaa003>
- Koenig-Robert, R., & Pearson, J. (2019). Decoding the contents and strength of imagery before volitional engagement. *Scientific Reports*, 9, 3504. <https://doi.org/10.1038/s41598-019-39813-y>
- LaRocque, J. J., Lewis-Peacock, J. A., Drysdale, A. T., Oberauer, K., & Postle, B. R. (2013). Decoding attended information in short-term memory: An EEG study. *Journal of Cognitive Neuroscience*, 25(1), 127–142. https://doi.org/10.1162/jocn_a_00305
- Lescroart, M. D., & Gallant, J. L. (2019). Human Scene-Selective Areas Represent 3D Configurations of Surfaces. *Neuron*, 101(1), 178–192.e7. <https://doi.org/10.1016/j.neuron.2018.11.004>
- Liu, S., Yu, Q., Tse, P. U., & Cavanagh, P. (2019). Neural Correlates of the Conscious Perception of Visual Location Lie Outside Visual Cortex. *Current Biology*, 29(23), 4036–4044.e4. <https://doi.org/10.1016/j.cub.2019.10.033>
- Long, N. M., & Kuhl, B. A. (2019). Decoding the tradeoff between encoding and retrieval to predict memory for overlapping events. *NeuroImage*, 201, 116001. <https://doi.org/10.1016/j.neuroimage.2019.07.014>
- Luck, S. J., & Vogel, E. K. (1997). The capacity of visual working memory for features and conjunctions. *Nature*, 390, 279–281. <https://doi.org/10.1038/36846>
- Luck, S. J., & Vogel, E. K. (2013). Visual working memory capacity: From psychophysics and neurobiology to individual differences. In *Trends in Cognitive Sciences* (Vol. 17, Issue 8, pp. 391–400). Elsevier Current Trends. <https://doi.org/10.1016/j.tics.2013.06.006>
- Luria, R., & Vogel, E. K. (2011). Shape and color conjunction stimuli are represented as bound objects in visual working memory. *Neuropsychologia*, 49(6), 1632–1639. <https://doi.org/10.1016/j.neuropsychologia.2010.11.031>
- Mares, I., Ewing, L., Farran, E. K., Smith, F. W., & Smith, M. L. (2020). Developmental changes in the processing of faces as revealed by EEG

- decoding. *NeuroImage*, 211, 116660.
<https://doi.org/10.1016/j.neuroimage.2020.116660>
- Maunsell, J. H. R., & Treue, S. (2006). Feature-based attention in visual cortex. In *Trends in Neurosciences* (Vol. 29, Issue 6, pp. 317–322). Elsevier Current Trends. <https://doi.org/10.1016/j.tins.2006.04.001>
- Nee, D. E., Brown, J. W., Askren, M. K., Berman, M. G., Demiralp, E., Krawitz, A., & Jonides, J. (2013). A meta-Analysis of executive components of working memory. *Cerebral Cortex*, 23(2), 264–282.
<https://doi.org/10.1093/cercor/bhs007>
- Noah, S., Powell, T., Khodayari, N., Olivan, D., Ding, M., & Mangun, G. R. (2020). Neural Mechanisms of Attentional Control for Objects: Decoding EEG Alpha When Anticipating Faces, Scenes, and Tools. *Journal of Neuroscience*, 40(25), 4913–4924.
<https://doi.org/10.1523/JNEUROSCI.2685-19.2020>
- Norman, K. A., Polyn, S. M., Detre, G. J., & Haxby, J. V. (2006). Beyond mind-reading: multi-voxel pattern analysis of fMRI data. In *Trends in Cognitive Sciences* (Vol. 10, Issue 9, pp. 424–430). Elsevier Current Trends. <https://doi.org/10.1016/j.tics.2006.07.005>
- Olson, I. R., & Jiang, Y. (2002). Is visual short-term memory object based? Rejection of the “strong-object” hypothesis. *Perception and Psychophysics*, 64(7), 1055–1067. <https://doi.org/10.3758/BF03194756>
- Parra, M. A., Cubelli, R., & della Sala, S. (2011). Lack of color integration in visual short-term memory binding. *Memory and Cognition*, 39(7), 1187–1197. <https://doi.org/10.3758/s13421-011-0107-y>
- Pedregosa, F., Varoquaux, G., Gramfort, A., Michel, V., Thirion, B., Grisel, O., Blondel, M., Prettenhofer, P., Weiss, R., Dubourg, V., Vanderplas, J., Cournapeau, D., Passos, A., Brucher, M., Perrot, M., & Duchesnay, M. (2011). Scikit-learn: Machine Learning in Python. In *Machine Learning in Python. Journal of Machine Learning Research* (Vol. 12). Microtome Pub-lishing. <https://hal.inria.fr/hal-00650905v2>
- Pertsov, Y., & Husain, M. (2014). The privileged role of location in visual working memory. *Attention, Perception, and Psychophysics*, 76(7), 1914–1924. <https://doi.org/10.3758/s13414-013-0541-y>
- Quentin, R., King, J. R., Sallard, E., Fishman, N., Thompson, R., Buch, E. R., & Cohen, L. G. (2019). Differential brain mechanisms of selection and maintenance of information during working memory. *Journal of Neuroscience*, 39(19), 3728–3740.
<https://doi.org/10.1523/JNEUROSCI.2764-18.2019>
- Quinlan, P. T., & Cohen, D. J. (2011). Object-based representations govern both the storage of information in visual short-term memory and the retrieval of information from it. *Psychonomic Bulletin and Review*, 18(2), 316–323. <https://doi.org/10.3758/s13423-011-0064-2>
- Rahmati, M., DeSimone, K., Curtis, C. E., & Sreenivasan, K. K. (2020).

- Spatially specific working memory activity in the human superior colliculus. *Journal of Neuroscience*, 40(49), 9487–9495.
<https://doi.org/10.1523/JNEUROSCI.2016-20.2020>
- Rahmati, M., Saber, G. T., & Curtis, C. E. (2018). Population dynamics of early visual cortex during working memory. *Journal of Cognitive Neuroscience*, 30(2), 219–233. https://doi.org/10.1162/jocn_a_01196
- Reddy, L., Tsuchiya, N., & Serre, T. (2010). Reading the mind's eye: Decoding category information during mental imagery. *NeuroImage*, 50(2), 818–825. <https://doi.org/10.1016/j.neuroimage.2009.11.084>
- Riggall, A. C., & Postle, B. R. (2012). The relationship between working memory storage and elevated activity as measured with functional magnetic resonance imaging. *Journal of Neuroscience*, 32(38), 12990–12998. <https://doi.org/10.1523/JNEUROSCI.1892-12.2012>
- Riggs, K. J., Simpson, A., & Potts, T. (2011). The development of visual short-term memory for multifeature items during middle childhood. *Journal of Experimental Child Psychology*, 108(4), 802–809.
<https://doi.org/10.1016/j.jecp.2010.11.006>
- Robinson, A. K., Grootswagers, T., & Carlson, T. A. (2019). The influence of image masking on object representations during rapid serial visual presentation. *NeuroImage*, 197, 224–231.
<https://doi.org/10.1016/j.neuroimage.2019.04.050>
- Schlegel, A., Kohler, P. J., Fogelson, S. V., Alexander, P., Konuthula, D., & Tse, P. U. (2013). Network structure and dynamics of the mental workspace. *Proceedings of the National Academy of Sciences of the United States of America*, 110(40), 16277–16282.
<https://doi.org/10.1073/pnas.1311149110>
- Serences, J. T., Ester, E. F., Vogel, E. K., & Awh, E. (2009). Stimulus-specific delay activity in human primary visual cortex. *Psychological Science*, 20(2), 207–214. <https://doi.org/10.1111/j.1467-9280.2009.02276.x>
- Shatek, S. M., Grootswagers, T., Robinson, A. K., & Carlson, T. A. (2019). Decoding images in the mind's eye: The temporal dynamics of visual imagery. *Vision (Switzerland)*, 3(4), 53.
<https://doi.org/10.3390/vision3040053>
- Shen, M., Tang, N., Wu, F., Shui, R., & Gao, Z. (2013). Robust object-based encoding in visual working memory. *Journal of Vision*, 13(2), 1–1.
<https://doi.org/10.1167/13.2.1>
- Shin, H., & Ma, W. J. (2016). Crowdsourced single-trial probes of visual working memory for irrelevant features. *Journal of Vision*, 16(5), 10–10.
<https://doi.org/10.1167/16.5.10>
- Smith, F. W., & Smith, M. L. (2019). Decoding the dynamic representation of facial expressions of emotion in explicit and incidental tasks. *NeuroImage*, 195, 261–271.
<https://doi.org/10.1016/j.neuroimage.2019.03.065>
- Stansbury, D. E., Naselaris, T., & Gallant, J. L. (2013). Natural Scene

- Statistics Account for the Representation of Scene Categories in Human Visual Cortex. *Neuron*, 79(5), 1025–1034.
<https://doi.org/10.1016/j.neuron.2013.06.034>
- Stokes, M., Thompson, R., Cusack, R., & Duncan, J. (2009). Top-down activation of shape-specific population codes in visual cortex during mental imagery. *Journal of Neuroscience*, 29(5), 1565–1572.
<https://doi.org/10.1523/JNEUROSCI.4657-08.2009>
- Swan, G., Collins, J., & Wyble, B. (2016). Memory for a single object has differently variable precisions for relevant and irrelevant features. *Journal of Vision*, 16(3), 32–32. <https://doi.org/10.1167/16.3.32>
- Treisman, A. M., & Gelade, G. (1980). A feature-integration theory of attention. *Cognitive Psychology*, 12(1), 97–136.
[https://doi.org/10.1016/0010-0285\(80\)90005-5](https://doi.org/10.1016/0010-0285(80)90005-5)
- Treisman, A., & Zhang, W. (2006). Location and binding in visual working memory. *Memory and Cognition*, 34(8), 1704–1719.
<https://doi.org/10.3758/BF03195932>
- Utochkin, I. S., & Brady, T. F. (2019). Independent Storage of Different Features of Real-World Objects in Long-Term Memory. *Journal of Experimental Psychology: General*, 149(3), 530–549.
<https://doi.org/10.1037/xge0000664>
- van Ede, F., Niklaus, M., & Nobre, A. C. (2017). Temporal Expectations Guide Dynamic Prioritization in Visual Working Memory through Attenuated α Oscillations. *The Journal of Neuroscience*, 37(2), 437–445.
<https://doi.org/10.1523/jneurosci.2272-16.2017>
- Vetter, P., Smith, F. W., & Muckli, L. (2014). Decoding sound and imagery content in early visual cortex. *Current Biology*, 24(11), 1256–1262.
<https://doi.org/10.1016/j.cub.2014.04.020>
- Vogel, E. K., Woodman, G. F., & Luck, S. J. (2001). Storage of features, conjunctions, and objects in visual working memory. *Journal of Experimental Psychology: Human Perception and Performance*, 27(1), 92–114. <https://doi.org/10.1037/0096-1523.27.1.92>
- Wheeler, M. E., & Treisman, A. M. (2002). Binding in short-term visual memory. *Journal of Experimental Psychology: General*, 131(1), 48–64.
<https://doi.org/10.1037/0096-3445.131.1.48>
- Wolff, M. J., Ding, J., Myers, N. E., & Stokes, M. G. (2015). Revealing hidden states in visual working memory using electroencephalography. *Frontiers in Systems Neuroscience*, 9(september), 123.
<https://doi.org/10.3389/fnsys.2015.00123>
- Woodman, G. F., & Vogel, E. K. (2008). Selective storage and maintenance of an object's features in visual working memory. *Psychonomic Bulletin and Review*, 15(1), 223–229. <https://doi.org/10.3758/PBR.15.1.223>
- Worden, M. S., Foxe, J. J., Wang, N., & Simpson, G. V. (2000). Anticipatory biasing of visuospatial attention indexed by retinotopically specific alpha-band electroencephalography increases over occipital cortex. *The*

Journal of Neuroscience : The Official Journal of the Society for Neuroscience, 20(6), RC63. <https://doi.org/10.1523/jneurosci.20-06-j0002.2000>

- Xie, S., Kaiser, D., & Cichy, R. M. (2020). Visual Imagery and Perception Share Neural Representations in the Alpha Frequency Band. *Current Biology*, 30(13), 2621-2627.e5. <https://doi.org/10.1016/j.cub.2020.04.074>
- Xu, Y. (2002). Limitations of object-based feature encoding in visual short-term memory. *Journal of Experimental Psychology: Human Perception and Performance*, 28(2), 458–468. <https://doi.org/10.1037/0096-1523.28.2.458>
- Yin, J., Zhou, J., Xu, H., Liang, J., Gao, Z., & Shen, M. (2012). Does high memory load kick task-irrelevant information out of visual working memory? *Psychonomic Bulletin and Review*, 19(2), 218–224. <https://doi.org/10.3758/s13423-011-0201-y>
- Zhan, J., Ince, R. A. A., van Rijsbergen, N., & Schyns, P. G. (2019). Dynamic Construction of Reduced Representations in the Brain for Perceptual Decision Behavior. *Current Biology*, 29(2), 319-326.e4. <https://doi.org/10.1016/j.cub.2018.11.049>

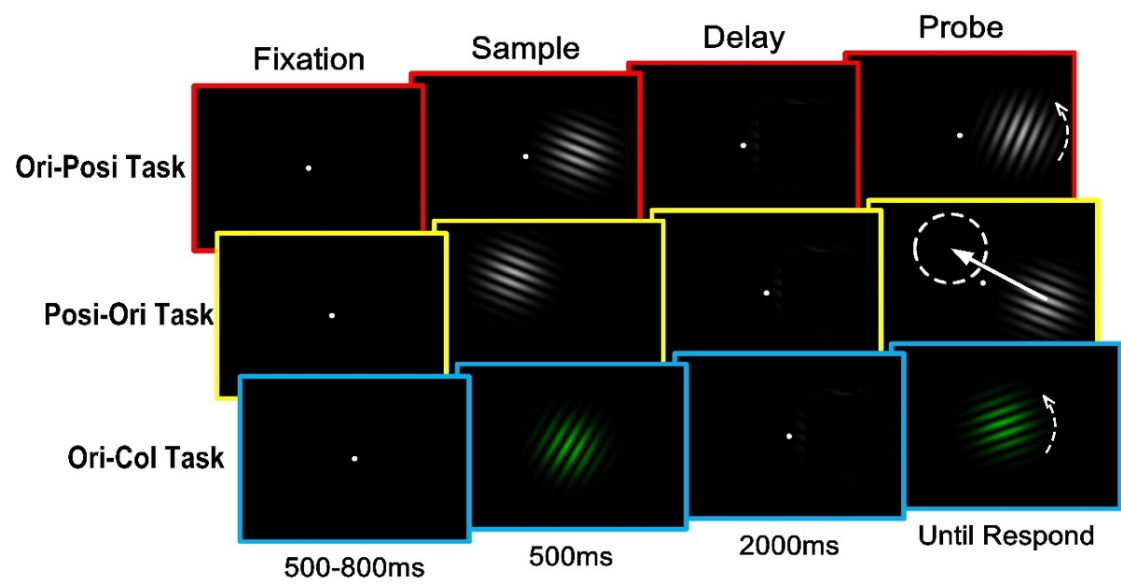


Figure 1. Trial sequence in three tasks.

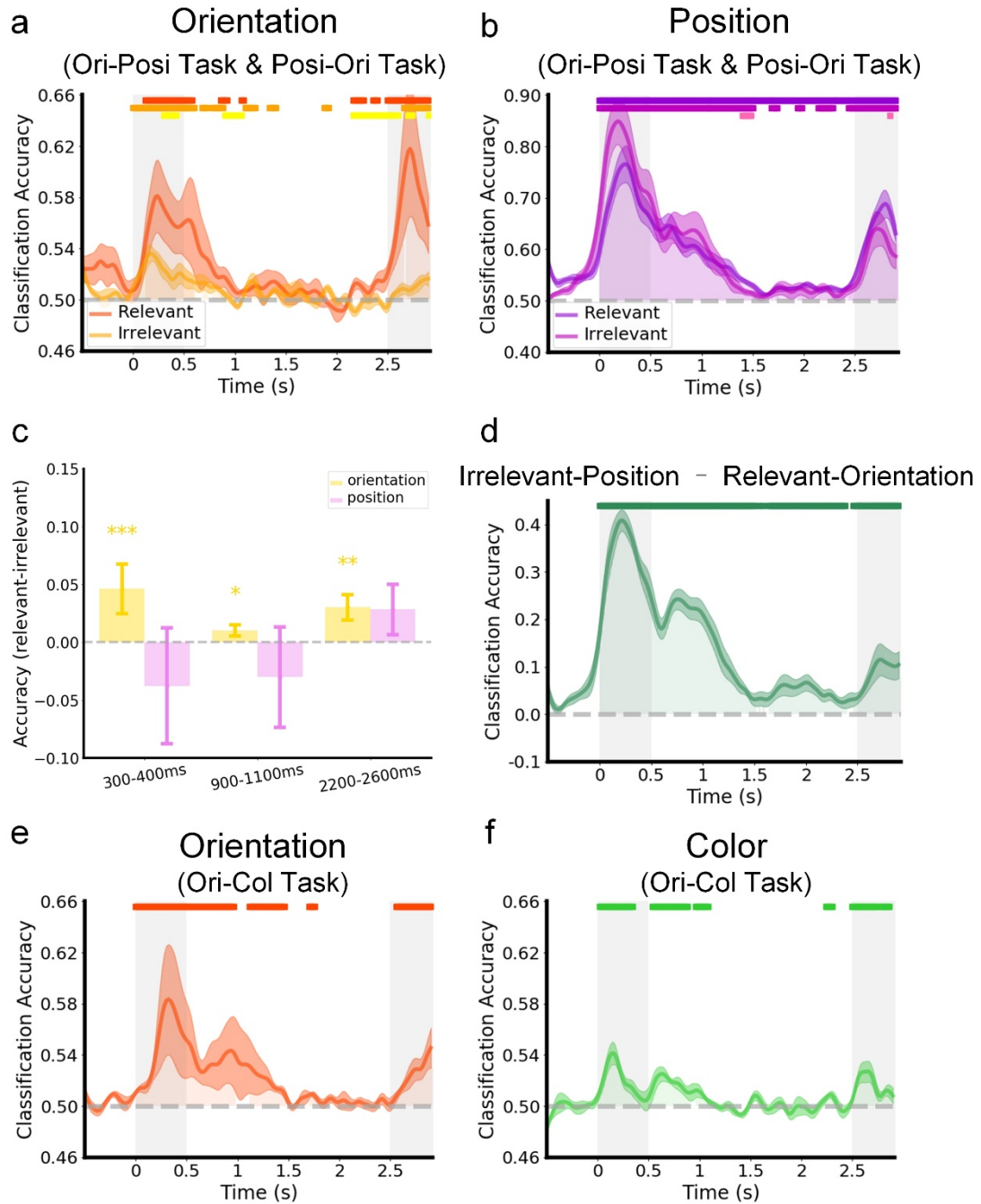


Figure 2. Time-by-time decoding accuracies. a) Decoding results for orientation as the relevant feature in task 1 and as the irrelevant feature in task 2. b) Decoding results for position as the relevant feature in task 2 and irrelevant feature in task 1. c) The differences in decoding accuracies of orientation and position between task-relevant and task-irrelevant during three time periods (300-400ms, 900-1100ms, and 2200-2600ms). d) Differences of decoding accuracies between the task-irrelevant position and the task-relevant orientation. e) Decoding results for orientation in task 3. f) Decoding results for color in task 3. The baseline of classification accuracy is 50%. Gray shadow represents the stimulus period and response period. The curve shows the average accuracies and the light shadow of the curve indicates \pm SEM. The upper square points and light color area indicate the time point significantly higher than the random level (permutation test, $p < 0.05$).

The baseline of classification accuracy is 50% in (a), (b), (e) and (f). In (a), (b), (d), (e) and (f), gray shadow represents the stimulus period and response period. The curve shows the average differences and the light shadow of the curve indicates \pm SEM. The square points indicate the time point that decoding accuracies between the task-irrelevant position and task-relevant orientation are significantly different (permutation test, $p < 0.05$). * $p < 0.05$, ** $p < 0.01$, *** $p < 0.001$.

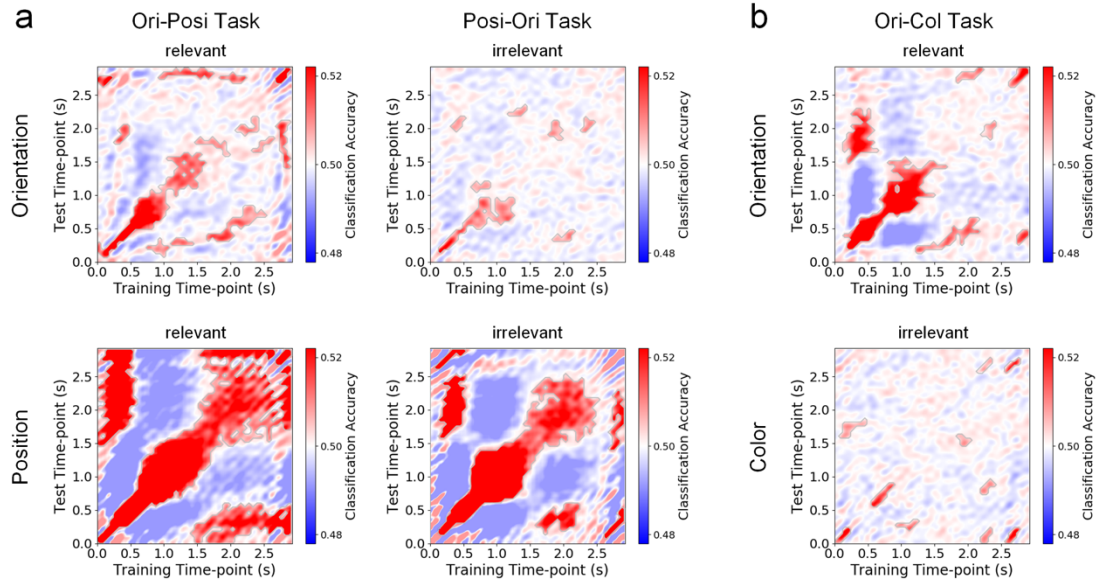


Figure 3. Temporal generalization decoding results. a) Cross-temporal decoding results for orientation and position in task 1 and task 2. b) Cross-temporal decoding results for orientation and color in task 3. These matrices show the average classification accuracy corresponding to a training time-point and a test time-point across all pairwise comparisons. The light grey outline indicates that the average accuracy is significantly higher than chance (cluster-based permutation test, $p < 0.01$).

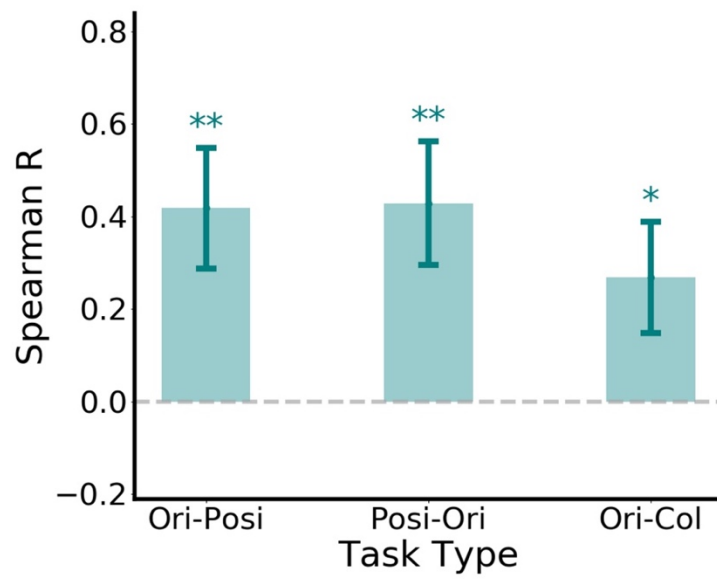


Figure 4. Correlations of decoding accuracies between the task-relevant and task-irrelevant features. The correlation coefficients were calculated based on Spearman Correlation. * $p < 0.05$, ** $p < 0.01$.

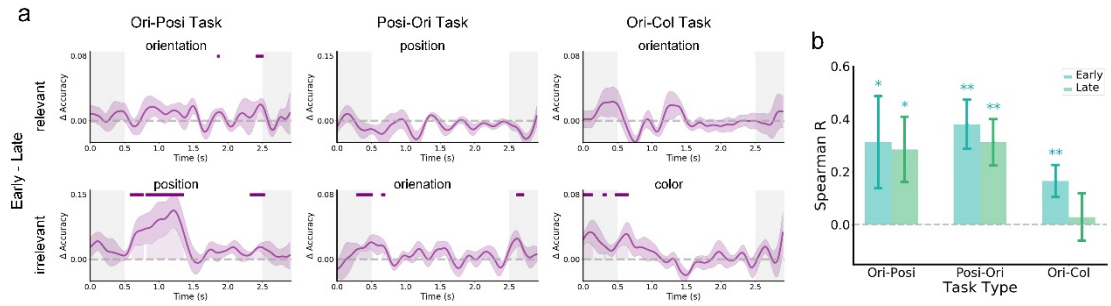


Figure 5. Phased decoding results. a) Differences between the classification performances of the two phases. The top shows the result for the task-relevant feature, and the bottom shows the results for the task-irrelevant feature—three tasks from left to right. The curves below show the differences time-by-time. The upper square points and light color area in curves indicate the time point significantly higher than the random level (permutation test, $p < 0.05$). b) Correlations of decoding accuracies computed on trials of the two phases. The correlation coefficients were calculated based on Spearman Correlation. * $p < 0.05$, ** $p < 0.01$.

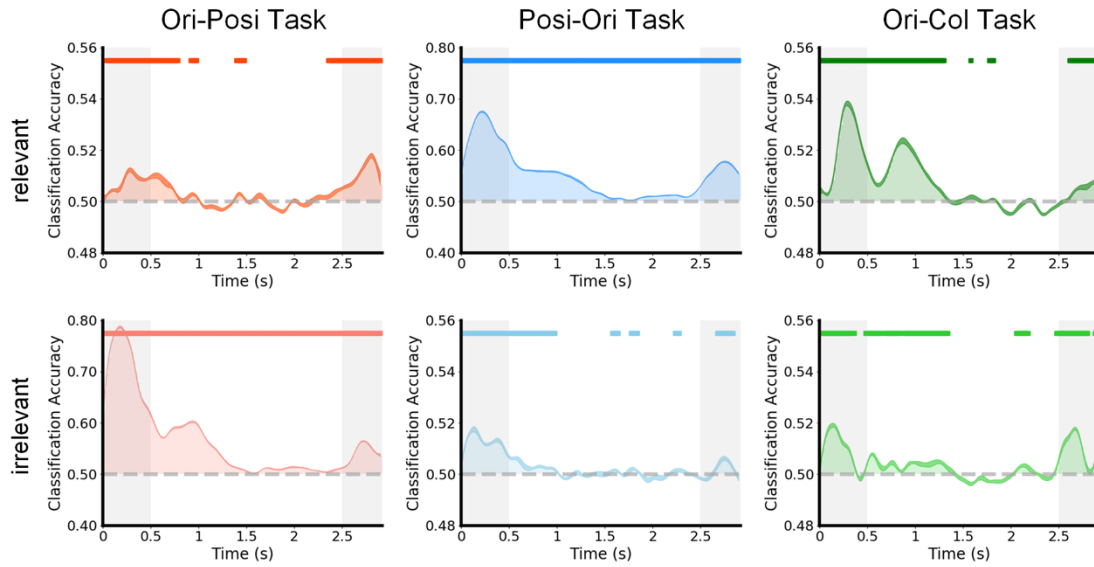


Figure 6. Across-participants decoding accuracy. The baseline of classification accuracy is 50%. Gray shadow represents the stimulus period and response period. The curve shows the average accuracy and the light shadow of the curve indicates \pm SEM. The upper square points and light color area indicate the time point significantly higher than the random level ($p < 0.001$).

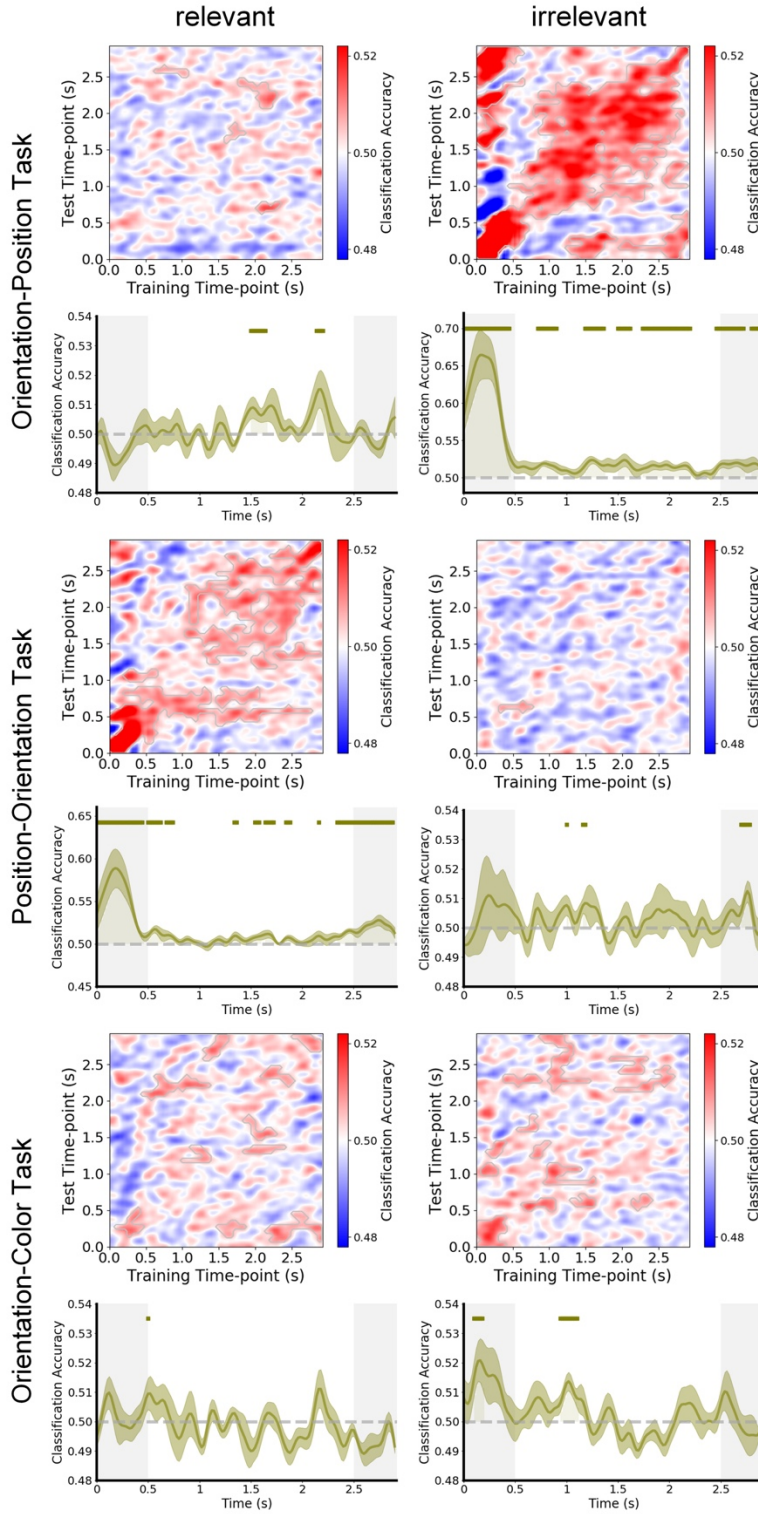


Figure 7. Alpha power decoding accuracy. Results for each term decoding include a temporal generalization matrix (above) by cross-temporal decoding and a curve (below) by time-by-time decoding. The above shows the classification performance of the attended feature and the below shows the classification performance of the unattended feature. The curves below show the average classification accuracy by time-by-time decoding. Three tasks from left to right. The matrices above show the average classification accuracy corresponding to a training time-point and a test time-point across all pairwise comparisons. Light grey outline

indicates that the average accuracy is significantly higher than chance (cluster-based permutation test, $p < 0.01$). The gray shadow in diagrams of curve represents the stimulus period and response period. The curve shows the average accuracy and the light shadow of the curve indicates \pm SEM. The upper square points and light color area of the curve indicate the time point significantly higher than the random level (permutation test, $p < 0.05$).